Soft Matter

Accepted Manuscript

ROYAL SOCIETY OF CHEMISTRY

www.rsc.org/softmatter

Effect of a capillary bridge on the crack opening of a penny crack

Fuqian Yang [1] and Ya-Pu Zhao [2]

1) Materials Program, Department of Chemical and Materials Engineering
University of Kentucky, Lexington, KY 40506

2) State Key Laboratory of Nonlinear Mechanics, Institute of Mechanics
Chinese Academy of Sciences, Beijing 100190, China

fyang2@uky.edu

Abstract

Young's relation is based on the equilibrium of the horizontal components of surface tensions for a liquid droplet on a "rigid" substrate without addressing the substrate deformation induced by the net vertical component of the surface tensions. Realizing the importance of wetting in controlling the integrity of flexible structures and electronics, the effect of a capillary bridge or a liquid droplet on the crack opening of a penny crack under the action of a far-field tensile stress is analyzed. Closed-form solutions are derived for both the crack opening and the stress intensity factor, which are functions of the size of the capillary bridge or droplet, surface tension, and contact angle. Both the capillary bridge and the droplet can introduce the crack closure. The minimum far-field tensile stresses needed for complete crack opening, i.e. no crack closure, are obtained analytically. The net vertical component of the surface tensions introduces the formation of a surface ridge on the crack face at the edge of the droplet for an open crack. The amplitude of the surface ridge increases with the increase of the net vertical component of the surface tensions and the decrease of the breadth width.

1. Introduction

The progress in the fabrication of flexible structures and electronics has been based on the use of soft matter, such as polymers. The use of soft matter has imposed a challenge in controlling structural integrity, even though soft matter can provide good biocompatibility and nontoxicity in the applications of biofluidics [1, 2] and bio-microelectromechanical structures [3, 4]. Generally, soft matter has a Young's modulus of a few MPa or lower, which makes soft matter easily deform even with the presence of a tiny, liquid droplet on the surface.

It is known that Young's relationship is derived under the equilibrium condition of the horizontal components of surface tensions for a liquid droplet on a "rigid" substrate, on which there are no chemical reactions. In analyzing the relationship between contact angles and surface tensions, Lester [5] pointed out that Young's equation is only applicable to nondeformable solid surfaces and introduced an average mean stress acting vertically on the solid surface at the edge of a droplet. Following Lester's approach [5], Rusanov [6] derived analytical expressions of the surface profile of an elastic half-space induced by a sessile droplet. Yu and Zhao [7] extended Rusanov's analysis [6] to the deformation of an elastic layer. Based on Métois' observation [8] that a liquid droplet on a thin graphite sheet introduces a deformed liquid/graphite interface, Kern and Müller [9] analyzed the droplet-induced deformation of an elastic thin film. However, there are seldom studies addressing the effect of liquid bridges or liquid droplets on the crack opening and stress intensity factors of cracks, which is associated with the capillary-assisted contact adhesion of solid surfaces.

Recently, there have been more studies [10-18] focusing on the droplet-induced deformation of soft matter with the aim of understanding local deformation around a contact line on soft polymers. Style et al. [19] used confocal microscopy to observe local deformation near the contact line for a glycerol or fluorinated-oil droplet on a silicone gel substrate and revealed the dependence of the deformed topology on the balance of interfacial tensions at the contact line. Marchand et al. [20] suggested that Young's relationship becomes invalid for analyzing the capillary-induced surface deformation of a soft substrate and proposed an elastocapillary model for contact angles on a soft solid by coupling a mean-field model for the molecular interactions to elasticity. Park et al. [21] observed the bending of an asymmetric tip during ridge growth associated with the wetting of a water droplet on a silicone gel and a PDMS film and suggested that it is surface stresses that determine the balance at the tip. Karpitschka et al. [22] used

Neumann's law to analyze the stick-slip motion of a droplet on a viscoelastic substrate. In analyzing the effect of surface stresses on the capillary-induced surface deformation, Style and Dufresne [23] suggested that it is the interfacial tensions instead of bulk elasticity that determine the shape of a solid substrate near the tip of a wetting ridge. In general, the effect of the surface tension/stresses on the local deformation at the contact edge is dependent on the ratio of the characteristic length to electrocapillary length.

Liquid bridges and liquid droplets play an important role in determining the performance of microfluidics and flexible electronics and the contact adhesion of solid surfaces. Recognizing that adhesive contact between solid surfaces is related to mode I crack, Maugis et al. [24] showed the connection between the JKR theory and the Griffith theory. In general, the capillary-related contact adhesion of solid surfaces involves the capillary-induced deformation and crack-like stress state. Young's equation [25] does not lead to the equilibrium of surface tensions, and the unbalanced surface tensions can result in local deformation of materials. One needs to consider the deformation of mechanical structures induced by a capillary bridge or a droplet in order to understand the structural integrity associated with contact adhesion.

This work aims to investigate the effect of a liquid bridge or a liquid droplet on the crack opening and stress intensity factor of a penny crack. Following Lester's approach [5], uniform stress in an annular zone of a breadth width in the triple-phase line is used, in addition to the normal stress induced by the liquid bridge/droplet on each individual crack face. The total force due to the uniform stress in the annular zone is equivalent to the net vertical component of the surface tensions.

2. Problem formulation

Consider a penny crack of radius c in an infinite space, as shown in Fig. 1. A capillary bridge of radius a joins the top surface of the crack with the bottom surface. The penny crack is subjected to a far-field tensile loading. Here cylindrical polar coordinates (r, ϕ, z) are used such that the $z-$axis coincides with the axis of the loading direction, the r -axis is perpendicular to the $z-$axis, and θ is the angular distance between a reference line and the r -axis. The nonzero displacements corresponding to the coordinates (r,ϕ,z) are u_r and u_z, which satisfy the following equations [26, 27]:

$$\nabla^2 u_r + \frac{1}{1-2\nu}\frac{\partial \Xi}{\partial r} - \frac{u_r}{r^2} = 0 \qquad (1)$$

$$\nabla^2 u_z + \frac{1}{1-2\nu}\frac{\partial \Xi}{\partial z} = 0 \tag{2}$$

$$\nabla^2 \Xi = 0 \tag{3}$$

$$\Xi = \frac{\partial u_r}{\partial r} + \frac{u_r}{r} + \frac{\partial u_z}{\partial z} \tag{4}$$

where the displacement vector $\vec{u} = u_r \vec{r} / |\vec{r}| + u_z \vec{z} / |\vec{z}|$ and Ξ is the dilation. The components of the stress tensor, σ_{ij}, in terms of the components of the displacement vector are

$$\sigma_{rr} = \lambda \Xi + 2\mu \frac{\partial u_r}{\partial r} \tag{5}$$

$$\sigma_{\theta\theta} = \lambda \Xi + 2\mu \frac{u_r}{r} \tag{6}$$

$$\sigma_{zz} = \lambda \Xi + 2\mu \frac{\partial u_z}{\partial z} \tag{7}$$

$$\sigma_{rz} = \mu \left(\frac{\partial u_r}{\partial z} + \frac{\partial u_z}{\partial r} \right) \tag{8}$$

where ν is the Poisson ratio, and λ and μ are the Lame constants.

For the penny-shaped crack being subjected to a far-field tensile stress, the boundary conditions are

$$\sigma_{zz} = \sigma_0 \qquad \text{for } |z| \to \infty \tag{9}$$

$$\sigma_{rz}(r, 0) = 0 \tag{10}$$

Equation (10) assumes that there is no friction between two crack surfaces and no tangential stress applied to the crack surfaces. Due to the symmetry, the displacement at the plane z = 0 satisfies

$$u_z = 0 \qquad \text{for } r > c \tag{11}$$

According to the theory of linear elasticity, the reference state of the structure is the stress-free (un-deformed) state. At the contact line between the liquid bridge and the crack surface at the reference state, Young's equation [25] gives the contact angle, θ, at the contact line as

$$\cos\theta = \frac{\gamma_{sv} - \gamma_{sl}}{\gamma_{lv}} \tag{12}$$

where γ_{lv} , γ_{sv} , and γ_{sl} , and are the interface tensions of the liquid/vapor, solid/vapor and solid/liquid interfaces, respectively. Equation (12) represents the force balance only along the tangential direction on the liquid/vapor and solid/liquid interfaces, which validates Eq. (10) if there is no friction between two crack surfaces. The net normal component of the surface tensions, acting on the contact line, must be balanced by the mechanical deformation inside solid.

There are various studies [7] addressing the mechanical deformation of solid induced by the net normal component of the surface tensions for a liquid droplet being placed on the surface of deformation materials. Lester [5] and Rusanov [6] suggested that there was a breadth of δ at the liquid–vapor interface and the liquid/vapor interface tension uniformly distributed over a narrow annulus in studying the deformation of an elastic half-space induced by a sessile liquid droplet. Following the approach used by Lester [5] and Rusanov [6], the normal stress on the crack surface can be expressed as

$$\sigma_{zz}(r,0) \equiv f(r) = \begin{cases} -p & r < a \\ \chi & \text{for} \quad a < r < a+\delta \\ 0 & a+\delta < r < c \end{cases} \tag{13}$$

For a capillary bridge of thickness $2h$ and contact radius a between the capillary bridge and the crack face, which is confined between two crack surfaces, the pressure p is calculated as

$$p = \gamma_{lv}\left(\frac{1}{a} - \frac{\cos\theta}{h}\right) \tag{14}$$

and the stress over the narrow annulus is

$$\chi = \frac{\gamma_{lv}\sin\theta}{\delta} \tag{15}$$

For $\cos\theta > 0$ and $R\cos\theta < h$, the crack surface experiences compressive stress; otherwise, the crack surface experiences tensile stress. For $\cos\theta < 0$, the crack surface experiences compressive stress.

It is worth pointing out that surface stresses [23, 28-31] generally need to be incorporated in the boundary condition of (13) for the deformation due to the wetting of a liquid droplet of small size [23]. Here, no surface stresses are incorporated in the boundary condition of (13), since the use of surface stresses introduces a new parameter, whose value is needed to be determined. Note that Young's equation may have to be modified for sufficiently large elastocapillary number.

3. Crack opening and stress intensity factor

With the above equations, it is possible to analyze the stress distribution and the stress intensity factor. Before solving these equations, the following dimensionless parameters are introduced:

$$(\tilde{r},\tilde{z}) = (r,z)/c\,,\ (\tilde{u}_r,\tilde{u}_z) = (u_r,u_z)/c\,,\ \lambda = a/c\,,\text{ and }\ \tilde{\delta} = \delta/c \tag{16}$$

Using the axisymmetry of the crack problem and the properties of the Bessel functions, one can find the crack opening as

$$\Delta = u_z(\tilde{r},0^+) - u_z(\tilde{r},0^-) = \frac{8(1-\nu^2)c}{\pi E}\int_{\tilde{r}}^1 \frac{tdt}{\sqrt{t^2-\tilde{r}^2}}\int_0^1 \frac{[\sigma_0 - f(txc)]xdx}{\sqrt{1-x^2}} \quad \text{for } \tilde{r}<1 \tag{17}$$

and normal component of the stress field in front of the crack tip as

$$\sigma_{zz}(\tilde{r},0) = -\frac{2}{\pi}\int_0^\infty \varsigma J_0(\varsigma\tilde{r})d\varsigma\int_0^1 t\sin(\varsigma t)dt\int_0^1 \frac{x[\sigma_0 - f(txc)]}{\sqrt{1-x^2}}dx \qquad \text{for } \tilde{r}>1 \tag{18}$$

with $tx = \tilde{r}$. Eq. (18) can be further simplified to

$$\sigma_{zz}(\tilde{r},0) = -\frac{2}{\pi}\frac{1}{\tilde{r}}\frac{d}{d\tilde{r}}\int_0^1 \frac{t^2 q(t)}{\sqrt{\tilde{r}^2-t^2}}dt \qquad \text{for } \tilde{r}>1 \tag{19}$$

where

$$q(t) = \int_0^1 \frac{[\sigma_0 - f(txc)]x}{\sqrt{1-x^2}}dx \tag{20}$$

For detailed derivation, see the supplementary material.

To derive both the stress intensity factor and the crack opening with the function $f(r)$ of Eq. (13), we first consider the auxiliary problem that a penny crack of dimensionless radius 1 in an infinite elastic space is only subjected to uniform pressure of p_0 on the crack surface over a circular area of dimensionless radius b (b<1), i.e.

$$\sigma_{zz} = 0 \qquad \text{for } |z| \to \infty \tag{21}$$

$$\sigma_{zz}(\tilde{r},0) = f(\tilde{r}) = \begin{cases} -p_0 & \tilde{r} < b \\ 0 & b < \tilde{r} < 1 \end{cases} \qquad \text{for} \tag{22}$$

Define

$$\Delta_0 = \frac{8(1-\nu^2)cp_0}{\pi E} \tag{23}$$

Substituting Eq. (22) in Eqs. (17), one obtains the crack opening of the auxiliary problem as

$$\frac{\Delta^a}{\Delta_0} = \sqrt{1-\tilde{r}^2}(1-\sqrt{1-b^2}) + b(\mathbf{E}[\frac{\tilde{r}^2}{b^2}] - \mathrm{E}[\sin^{-1}b, \frac{\tilde{r}^2}{b^2}]) \qquad \text{for } \tilde{r}<b \tag{24}$$

$$\frac{\Delta^a}{\Delta_0}=\sqrt{1-\tilde{r}^2}\,(1-\sqrt{1-b^2}) \qquad \text{for } b<\tilde{r}<1 \qquad (25)$$

$$+\tilde{r}\left(\mathbf{E}[\frac{b^2}{\tilde{r}^2}]-\mathrm{E}[\sin^{-1}\tilde{r},\frac{b^2}{\tilde{r}^2}]+\left(1-\frac{b^2}{\tilde{r}^2}\right)\left(\mathrm{F}[\sin^{-1}\tilde{r},\frac{b^2}{\tilde{r}^2}]-\mathbf{K}[\frac{b^2}{\tilde{r}^2}]\right)\right)$$

Here $\Phi(\bullet,\bullet)$ and $\mathrm{E}(\bullet,\bullet)$ are the first and second elliptical integrals, respectively, and $\mathbf{E}(\bullet)$ and $\mathbf{K}(\bullet)$ are the first and the second complete elliptical integrals, respectively. Note that the $\tilde{r}/b$ and $b/\tilde{r}$ in the elliptical integrals in the work of Parihar and Krishna Rao [32] need to be replaced by $\tilde{r}^2/b^2$ and $b^2/\tilde{r}^2$, respectively. For $b\to 1$, there is

$$\Delta^a=\frac{4(1-\nu^2)cp_0}{\pi E}\frac{b^2}{\tilde{r}}\cos^{-1}\tilde{r}=\frac{4(1-\nu^2)c}{\pi^2 E}\frac{P}{\tilde{r}}\cos^{-1}\tilde{r} \qquad \text{for } b\to\ \tilde{r}<1 \qquad (26)$$

with P being the applied load. Figure 2 shows the crack opening for various b. Under the action of the same pressure, the largest crack opening occurs for b=1 and can be simply described by $\sqrt{1-\tilde{r}^2}$, as expected. In contrast to the case for b=1, the crack opening begins concave down, becomes concave up at the edge of the loading zone, and finally becomes concave down near the crack tip. This result reveals the dependence of the crack opening near the crack tip on the loading condition. For $\tilde{r}\to 1$, there is

$$\lim_{\tilde{r}\to 1}\frac{\Delta^a}{\Delta_0}=\sqrt{1-\tilde{r}^2}\,(1-\sqrt{1-b^2}) \qquad (27)$$

which reduces to the result for b=1.

The normal component of the stress field in front of the crack tip of the auxiliary problem is

$$\frac{\sigma^a_{zz}(\tilde{r},0)}{p_0}==\frac{2}{\pi}\left(\frac{1-\sqrt{1-b^2}}{\sqrt{\tilde{r}^2-1}}+\frac{\pi}{4}-\cot^{-1}(\sqrt{\tilde{r}^2-1})+\frac{1}{2}\tan^{-1}\frac{2-b^2-\tilde{r}^2}{2\sqrt{1-b^2}\sqrt{\tilde{r}^2-1}}\right) \qquad (28)$$

for $\tilde{r}>1$, which gives the same stress distribution as that by Parihar and Krishna Rao [32]. For $b\to 1$, there is

$$\frac{\sigma^a_{zz}(\tilde{r},0)}{p_0}=\frac{2}{\pi}\left(\frac{1}{2}\frac{b^2}{\tilde{r}^2}\left(\frac{1}{\sqrt{\tilde{r}^2-1}}-\frac{b}{\sqrt{\tilde{r}^2-b^2}}\right)+\frac{b}{\sqrt{\tilde{r}^2-b^2}}-\tan^{-1}\frac{b}{\sqrt{\tilde{r}^2-b^2}}\right) \qquad (29)$$

Equation (28) gives the stress intensity factor, K_I^a, as

$$K_I^a=\lim_{\tilde{r}\to 1}\sqrt{2\pi c(\tilde{r}-1)}\sigma_{zz}(\tilde{r},0)=2p_0(1-\sqrt{1-b^2})\sqrt{\frac{c}{\pi}} \qquad (30)$$

Here, the superscript a represents the auxiliary problem.

Using the principle of superposition, the crack problem with the boundary conditions of (9)-(13) can be solved from the following three sub-problems.

Sub-problem I:

The normal stress on the crack face is

$$\sigma_{zz}^{I}(\tilde{r},0) = -\sigma_0 \qquad \text{for } 0<\tilde{r}<1 \tag{31}$$

which represents uniform pressure applied on the crack face.

Sub-problem II:

The normal stress on the crack face is

$$\sigma_{zz}^{II}(\tilde{r},0) = \begin{cases} -(p+\chi) & \\ 0 & \end{cases} \qquad \text{for } \begin{matrix} \tilde{r}<\lambda \\ \lambda<\tilde{r}<1 \end{matrix} \tag{32}$$

Sub-problem III:

The normal stress on the crack face is

$$\sigma_{zz}^{II}(\tilde{r},0) = \begin{cases} \chi & \\ 0 & \end{cases} \qquad \text{for } \begin{matrix} \tilde{r}<\lambda+\tilde{\delta} \\ \lambda+\tilde{\delta}<\tilde{r}<1 \end{matrix} \tag{33}$$

The combination of the sub-problem II and III represents the pressure applied on the crack face due to the capillary bridge.

Define

$$\Delta_\sigma = \frac{8(1-\nu^2)c\sigma_0}{\pi E} \tag{34}$$

Using the results of the auxiliary problem, the crack opening is obtained as

$$\frac{\Delta^a}{\Delta_\sigma} = \sqrt{1-\tilde{r}^2}\left(1+\frac{p+\chi}{\sigma_0}(1-\sqrt{1-\lambda^2})-\frac{\chi}{\sigma_0}[1-\sqrt{1-(\lambda+\tilde{\delta})^2}]\right) \quad \text{for } \tilde{r}<\lambda \tag{35}$$

$$+\lambda\frac{p+\chi}{\sigma_0}(\mathbf{E}[\frac{\tilde{r}^2}{\lambda^2}]-\mathrm{E}[\sin^{-1}\lambda,\frac{\tilde{r}^2}{\lambda^2}])-(\lambda+\tilde{\delta})\frac{\chi}{\sigma_0}(\mathbf{E}[\frac{\tilde{r}^2}{(\lambda+\tilde{\delta})^2}]-\mathrm{E}[\sin^{-1}(\lambda+\tilde{\delta}),\frac{\tilde{r}^2}{(\lambda+\tilde{\delta})^2}])$$

$$\frac{\Delta^a}{\Delta_\sigma} = \sqrt{1-\tilde{r}^2}\left(1+\frac{p+\chi}{\sigma_0}(1-\sqrt{1-\lambda^2})-\frac{\chi}{\sigma_0}[1-\sqrt{1-(\lambda+\tilde{\delta})^2}]\right) \quad \text{for } \lambda<\tilde{r}<\lambda+\tilde{\delta} \tag{36}$$

$$+\tilde{r}\frac{p+\chi}{\sigma_0}\left(\mathbf{E}[\frac{\lambda^2}{\tilde{r}^2}]-\mathrm{E}[\sin^{-1}\tilde{r},\frac{\lambda^2}{\tilde{r}^2}]+\left(1-\frac{\lambda^2}{\tilde{r}^2}\right)\left(\mathrm{F}[\sin^{-1}\tilde{r},\frac{\lambda^2}{\tilde{r}^2}]-\mathbf{K}[\frac{\lambda^2}{\tilde{r}^2}]\right)\right)$$

$$-(\lambda+\tilde{\delta})\frac{\chi}{\sigma_0}(\mathbf{E}[\frac{\tilde{r}^2}{(\lambda+\tilde{\delta})^2}]-\mathrm{E}[\sin^{-1}(\lambda+\tilde{\delta}),\frac{\tilde{r}^2}{(\lambda+\tilde{\delta})^2}])$$

$$\frac{\Delta^a}{\Delta_\sigma}=\sqrt{1-\tilde{r}^2}\left(1+\frac{p+\chi}{\sigma_0}(1-\sqrt{1-\lambda^2})-\frac{\chi}{\sigma_0}[1-\sqrt{1-(\lambda+\tilde{\delta})^2}]\right) \quad \text{for } \lambda+\tilde{\delta}<\tilde{r}<1 \quad (37)$$

$$+\tilde{r}\frac{p+\chi}{\sigma_0}\left(\mathbf{E}[\frac{\lambda^2}{\tilde{r}^2}]-\mathrm{E}[\sin^{-1}\tilde{r},\frac{\lambda^2}{\tilde{r}^2}]+\left(1-\frac{\lambda^2}{\tilde{r}^2}\right)\left(\mathrm{F}[\sin^{-1}\tilde{r},\frac{\lambda^2}{\tilde{r}^2}]-\mathbf{K}[\frac{\lambda^2}{\tilde{r}^2}]\right)\right)$$

$$-\tilde{r}\frac{\chi}{\sigma_0}\left(\mathbf{E}[\frac{(\lambda+\tilde{\delta})^2}{\tilde{r}^2}]-\mathrm{E}[\sin^{-1}\tilde{r},\frac{(\lambda+\tilde{\delta})^2}{\tilde{r}^2}]+\left(1-\frac{(\lambda+\tilde{\delta})^2}{\tilde{r}^2}\right)\left(\mathrm{F}[\sin^{-1}\tilde{r},\frac{(\lambda+\tilde{\delta})^2}{\tilde{r}^2}]-\mathbf{K}[\frac{(\lambda+\tilde{\delta})^2}{\tilde{r}^2}]\right)\right)$$

and the stress intensity factor K_I as

$$K_I=2\sqrt{\frac{c}{\pi}}\sigma_0\left[1+\frac{\gamma_{lv}}{\sigma_0}\left(\frac{1}{a}-\frac{\cos\theta}{h}\right)(1-\sqrt{1-\left(\frac{a}{c}\right)^2})+\frac{\gamma_{lv}\sin\theta}{\sigma_0\delta}(\sqrt{1-\left(\frac{a+\delta}{c}\right)^2}-\sqrt{1-\left(\frac{a}{c}\right)^2})\right] \quad (38)$$

It is evident that the stress intensity factor is dependent on the surface tension of the liquid, the contact angle, the radius of the capillary bridge, and the thickness of the capillary bridge.

4. Numerical results and discussion

To illustrate the effect of the capillary bridge on the crack opening and the stress intensity factor, numerical calculation is carried out. Consider a water film confined in a penny crack of radius 1 μm in a soft material of PDMS (Polydimethylsiloxane). The Young's modulus of PDMS is ~1 MPa, and the contact angle is 120° [7]. The surface tension of water is 72 mN/m. There is no accurate value of the breadth width of a capillary layer currently available, and Yu and Zhao [7] had used the values of 1, 10, and 40 nm for δ in their analysis. Here, the values of 1, 10, and 40 nm for δ are used in the following calculation.

Figure 3 shows the crack opening under concurrent action of a capillary bridge and various far-field tensile stresses. The following parameters are used in the calculation: a= c/100, h=10 nm, and δ=1 nm. It is evident that the normal stress induced by the net vertical component of the surface tensions leads to the formation of local ridge similar to the local deformation induced by a sessile droplet. Without the action of a far-field tensile stress or with the action of a small far-field tensile stress, there exists overlap between two crack faces as shown in Fig. 3 for the numerical results with $\sigma_0=10$ Pa. This result suggests that the stress condition of (13) becomes invalid over the annular region of $a<r<a+\delta$, which should be replaced by a displacement condition, i.e. the capillary bridge causes the crack closure due to the net vertical component of the surface tensions. The size of the crack closure is also dependent on the size of the capillary bridge.

The smallest far-field tensile stress of σ_s^c to have the stress condition of (13) over the annular region of $a < r < a + \delta$ before the rupture of the capillary bridge can be calculated from $\Delta^a = 0$ and is

$$\sigma_s^c = \left[-\lambda(p+\chi)\left(1 - \mathrm{E}[\sin^{-1}\lambda, 1]\right) + (\lambda+\tilde{\delta})\chi(\mathbf{E}[\frac{\lambda^2}{(\lambda+\tilde{\delta})^2}] - \mathrm{E}[\sin^{-1}(\lambda+\tilde{\delta}), \frac{\lambda^2}{(\lambda+\tilde{\delta})^2}]) \right](1-\lambda^2)^{-1/2} \quad (39)$$

$$-(p+\chi)(1-\sqrt{1-\lambda^2}) + \chi[1-\sqrt{1-(\lambda+\tilde{\delta})^2}]$$

which is the function of the breadth width, the surface tension of the liquid, the contact angle and contact radius of the liquid on the crack face.

As shown in Fig. 3, the crack opening increases with the increase of the far-field tensile stress, as expected. The increase in the crack opening will eventually lead to the rupture of the capillary bridge and the formation of a droplet on each individual crack face. It is known that the total free energy of the system consists of the sum of the strain energy stored in the soft material, the volume energy stored in the liquid phase, the surface energy associated with the surface of the liquid phase, and the interface energy associated with the interface of the liquid and the soft material. The rupture of the liquid bridge will occur when the total free energy of the system with the liquid bridge is larger than that of the system with two liquid droplets of the same total volume as the liquid bridge.

After the rupture of the liquid bridge, assume that there are two identical liquid droplets of spherical cap formed on the crack faces, and there is only one liquid droplet on each individual crack face. The normal stress applied to the crack surface over the contact zone by the droplet becomes

$$\sigma_{zz}(\tilde{r}, 0) = -\gamma_{lv}\frac{2\sin\theta}{a} \qquad \text{for } \tilde{r} < \lambda \qquad (40)$$

and the stress intensity factor becomes

$$K_I = 2\sqrt{\frac{c}{\pi}}\sigma_0\left[1 + \frac{2\gamma_{lv}\sin\theta}{a\sigma_0}(1-\sqrt{1-\left(\frac{a}{c}\right)^2}) + \frac{\gamma_{lv}\sin\theta}{\sigma_0\delta}(\sqrt{1-\left(\frac{a+\delta}{c}\right)^2} - \sqrt{1-\left(\frac{a}{c}\right)^2})\right] \quad (41)$$

Note that the liquid droplet always introduces compressive stress on the crack face over the contact zone in contrast to the capillary bridge. The following discussion is mainly focused on the effect of the droplet on the deformation of the crack face.

Figure 4 shows the crack opening for three different contact angles and c=1 μm, a=c/10, δ=1 nm, and σ_0=0.15E. For $\tilde{r} > \lambda + \tilde{\delta}$, there is no significant difference in the crack opening for all the three contact angles, while, for the $\tilde{r} < \lambda$, the crack opening for $\theta = 90^o$ is larger than those for $\theta = 60^o$ and 120^o, as expected from Eq. (40). Over the annular zone of $\lambda < \tilde{r} < \lambda + \tilde{\delta}$, the crack opening for $\theta = 90^o$ is smaller than those for $\theta = 60^o$ and 120^o in accord with the condition of (15). The droplet induces the formation of a surface ridge at the edge of the droplet due to the net vertical component of the surface tensions. For a small far-field tensile stress, the droplet formed from the rupture of a capillary bridge can also lead to the crack closure near the edge of the droplet. The minimum far-field stress to have an opening crack without the crack closure due to the surface deformation around the edge of the droplet can be calculated from Eq. (39) by replacing p with the following equation

$$p = \gamma_{lv} \frac{2\sin\theta}{a} \tag{42}$$

Figure 5 shows the crack opening under concurrent action of a capillary bridge and a far-field tensile stress for three droplet sizes. The following parameters are used in the calculation: c=1 μm, δ=1 nm, σ_0=0.15E, and θ=60°. The crack opening for the region with $2\lambda < \tilde{r} < 1$ is independent of the droplet size for the conditions used in the calculation. In the region occupied by the droplet, the larger the droplet, the larger the crack opening is at the same position, even though the pressure acting on the crack face, as given in Eq. (42), is smaller. Such behavior is due to the synergetic effect of the pressure inside the droplet, which gives a larger normal force, F, for a larger droplet as

$$F = \pi a^2 p = 2\pi a \gamma_{lv} \sin\theta \tag{43}$$

However, the crack opening over the annular zone near the edge of the droplet decreases with increasing the droplet size. This result indicates that a larger far-field tensile stress is needed to prevent the occurrence of the crack closure for a larger droplet, which is in accord with the relationship between σ_s^c and λ in Eq. (39).

The effect of the breadth width on the crack opening over the annular zone near the edge of the droplet is depicted in Fig. 6. The following parameters are used in the calculation: c=1 μm, a=c/5, σ_0=0.15E, and θ=60°. The crack opening decreases with increasing the breadth width. Such behavior is due to the distribution of the same resultant force (the net vertical component of

the surface tensions) over an annular zone. The larger the annular zone, the smaller the normal stress is over the annular zone. Smaller normal stress will introduce smaller surface deformation on the crack surface.

5. Summary

In summary, the effect of a capillary bridge or a liquid droplet on the crack opening of a penny crack under the action of a far-field tensile stress was analyzed. Considering the unbalance of the surface tensions in the direction perpendicular to the crack face, the approach used by Lester [5] and Rusanov [6] was used to describe the capillary-induced normal stress over an annular zone of a breadth width at the edge of the capillary bridge and the liquid droplet. The crack opening and the distribution of normal stress in front of the crack tip as well as the Mode I stress intensity factor were derived analytically. The sizes of the capillary bridge and the droplet play an important role in determining both the crack opening and the stress intensity factor. Without or with the action of a small far-field tensile stress, there likely exists the crack closure, i.e. surface contact, induced by the net vertical component of the surface tensions for a capillary bridge between crack faces or a liquid droplet on the crack face. This result reveals the phenomenon of the capillary-induced contact of solid surfaces. With the increase of the far-field tensile stress, the capillary bridge will be ruptured, leading to the formation of a droplet on each individual crack face. The smallest far-field tensile stresses needed for complete crack opening, i.e. no crack closure, were obtained analytically for the capillary bridge and the droplet, respectively. Without the presence of the crack closure, the net vertical component of the surface tensions introduces the formation of a surface ridge on the crack face at the edge of the droplet. The amplitude of the surface ridge increases with the increase of the net vertical component of the surface tensions and the decrease of the breadth width, while it increases with the increase of the contact angle, reaches the maximum at the contact angle of 90º, and decreases with further increasing the contact angle. The analysis reveals the important role of capillary bridges and liquid droplets in controlling the performance and reliability of the mechanical structures made from soft matter and the capillary-induced contact of mechanical structures of small scales.

ACKNOWLEDGMENTS

The authors are grateful for the support of the “Opening fund of State Key Laboratory of Nonlinear Mechanics (LNM)”.

References:

1. J. A. Kim, J. Y. Lee, S. Seong, S. H. Cha, S. H. Lee, J. J. Kim and T. H. Park, *Biochem Eng J*, 2006, **29**, 91-97.
2. A. Gang, N. Haustein, L. Baraban and G. Cuniberti, *Rsc Adv*, 2015, **5**, 11806-11811.
3. K. Zhou, X. G. Zhu, Y. Li and J. Liu, *Rsc Adv*, 2014, **4**, 31988-31993.
4. G. C. Shao, J. H. Wu, Z. L. Cai and W. J. Wang, *Sensors Actuators a-Phys*, 2012, **178**, 230-236.
5. G. R. Lester, *J Coll Sci Imp U Tok*, 1961, **16**, 315-326.
6. A. I. Rusanov, *Colloid J USSR*, 1975, **37**, 614-622.
7. Y. S. Yu and Y. P. Zhao, *J Colloid Interf Sci*, 2009, **339**, 489-494.
8. J. J. Metois, *Surf Sci*, 1991, **241**, 279-288.
9. R. Kern and P. Muller, *Surf Sci*, 1992, **264**, 467-494.
10. N. Nadermann, C. Y. Hui and A. Jagota, *P Natl Acad Sci USA*, 2013, **110**, 10541-10545.
11. V. A. Lubarda, *Soft Matter*, 2012, **8**, 10288-10297.
12. R. Pericet-Camara, A. Best, H. J. Butt and E. Bonaccurso, *Langmuir*, 2008, **24**, 10565-10568.
13. J. Olives, *J Phys-Condens Mat*, 1993, **5**, 2081-2094.
14. H. J. Butt, W. J. P. Barnes, A. del Campo, M. Kappl and F. Schonfeld, *Soft Matter*, 2010, **6**, 5930-5936.
15. J. B. Bostwick, M. Shearer and K. E. Daniels, *Soft Matter*, 2014, **10**, 7361-7369.
16. K. Lia and S. Q. Cai, *Soft Matter*, 2014, **10**, 8202-8209.
17. J. S. Wexler, T. M. Heard and H. A. Stone, *Phys Rev Lett*, 2014, **112**, 066102.
18. C.-Y. Hui and A. Jagota, *Soft Matter*, 2015, **11**, 8960-8967.
19. R. W. Style, R. Boltyanskiy, Y. L. Che, J. S. Wettlaufer, L. A. Wilen and E. R. Dufresne, *Phys Rev Lett*, 2013, **110**, 066103.
20. A. Marchand, S. Das, J. H. Snoeijer and B. Andreotti, *Phys Rev Lett*, 2012, **109**, 236101.
21. S. J. Park, B. M. Weon, J. S. Lee, J. Lee, J. Kim and J. H. Je, *Nat Commun*, 2014, **5**, DOI: 10.1038/ncomms5369.
22. S. Karpitschka, S. Das, M. van Gorcum, H. Perrin, B. Andreotti and J. H. Snoeijer, *Nat Commun*, 2015, **6**, DOI: 10.1038/ncomms8891.
23. R. W. Style and E. R. Dufresne, *Soft Matter*, 2012, **8**, 7177-7184.
24. D. Maugis, M. Barquins and R. Courtel, *Metaux-Corrosion-Industrie*, 1976, 1-10.

25. T. Young, *Phil. Trans. R. Soc. Lond*, 1805, **95**, 65-87.
26. F. Q. Yang, *Mechanics of Materials*, 1998, **30**, 275-286.
27. F. Q. Yang, *Mat Sci Eng a-Struct*, 2003, **358**, 226-232.
28. J. Dervaux and L. Limat, *P Roy Soc a-Math Phy*, 2015, **471**, 20140813.
29. F. Q. Yang, *J Appl Phys*, 2006, **99**, 054306.
30. C. C. Lin, F. Q. Yang and S. Lee, *Langmuir*, 2008, **24**, 13627-13631.
31. C.-Y. Hui and A. Jagota, *Proc. Royal Soc London A: Math Phys Eng Sci*, 2014, 470, 20140085.
32. K. Parihar and J. K. Rao, *Engineering fracture mechanics*, 1991, **39**, 1067-1095.

Figure captions:

1. Schematic of a penny crack with a liquid bridge in an infinite space
2. Crack opening under the action of uniform pressure over a circular area of dimensionless radius b
3. Crack opening of the penny crack under concurrent action of a capillary bridge and a far-field tensile stress for three values of the tensile stress (c=1 μm, a=c/100, h=10 nm, δ=1 nm, θ=120°)
4. Crack opening of the penny crack under concurrent action of a droplet of radius c and a far-field tensile stress for three contact angles (c=1 μm, a=c/10, δ=1 nm, σ_0=0.15E)
5. Crack opening of the penny crack under concurrent action of a droplet and a far-field tensile stress for three droplet sizes (c=1 μm, δ=1 nm, σ_0=0.15E, θ=60°)
6. Crack opening of the penny crack under concurrent action of a droplet and a far-field tensile stress for three breadth widths (c=1 μm, a=c/5, σ_0=0.15E, θ=60°)

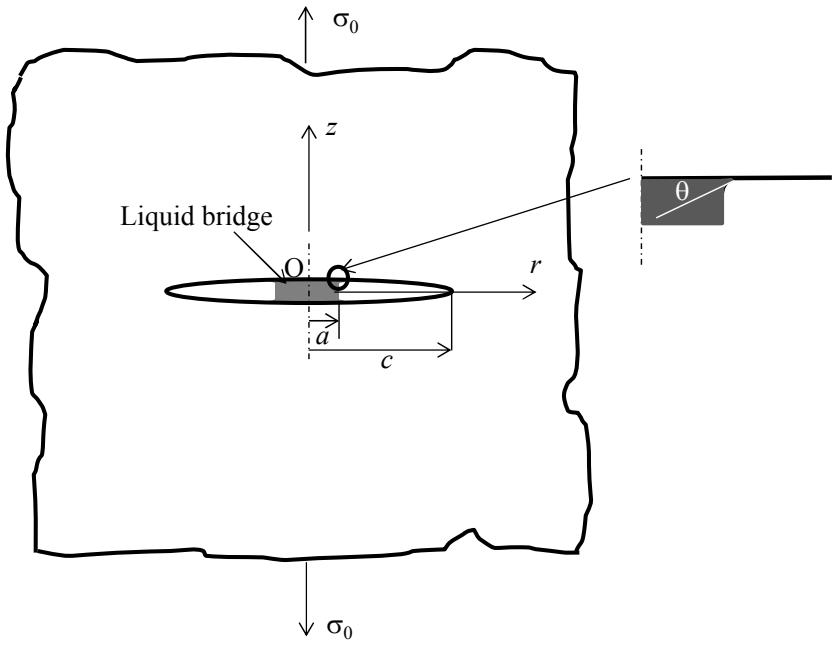

Figure 1. Schematic of a penny crack with a liquid bridge in an infinite space

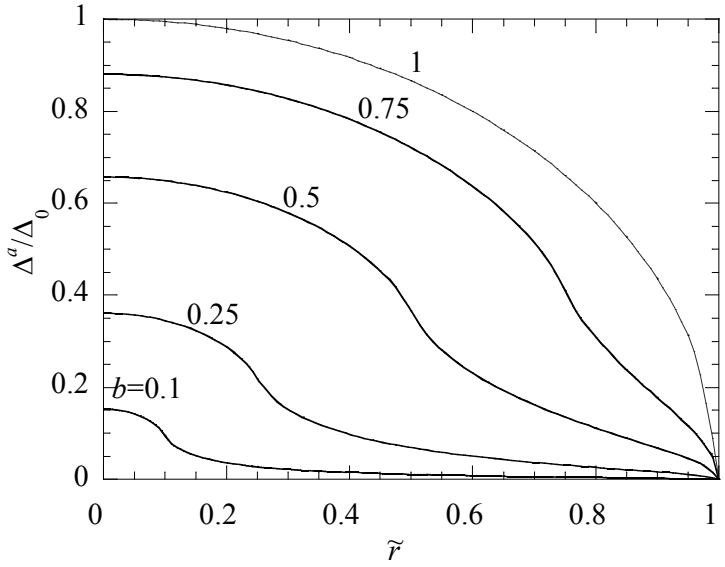

Figure 2. Crack opening under the action of uniform pressure over a circular area of dimensionless radius b

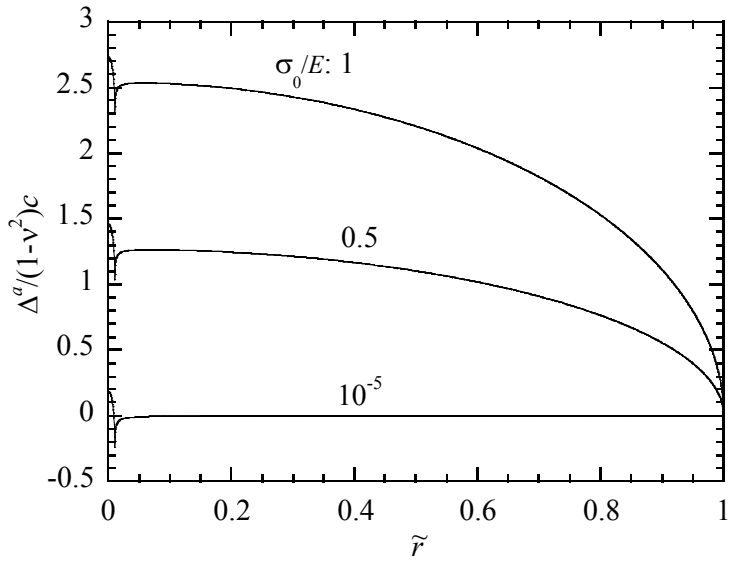

Figure 3. Crack opening of the penny crack under concurrent action of a capillary bridge and a far-field tensile stress for three values of the tensile stress (c=1 μm, a=c/100, h=10 nm, δ=1 nm, θ=120°)

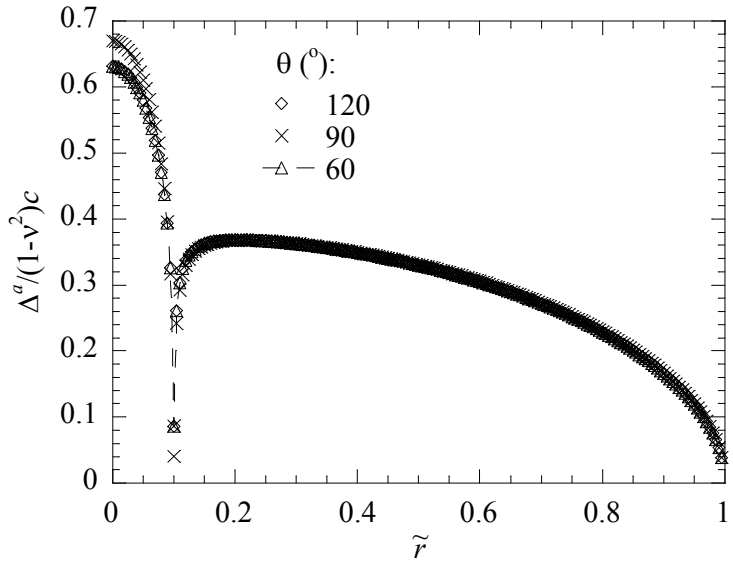

Figure 4. Crack opening of the penny crack under concurrent action of a droplet of radius c and a far-field tensile stress for three contact angles (c=1 μm, a=c/10, δ=1 nm, σ_0=0.15E)

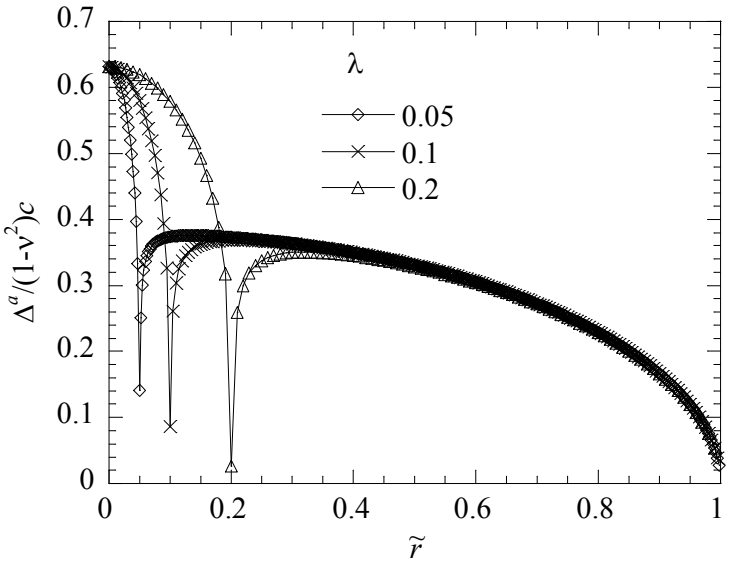

Figure 5. Crack opening of the penny crack under concurrent action of a droplet and a far-field tensile stress for three droplet sizes (c=1 μm, δ=1 nm, σ_0=0.15E, θ=60°)

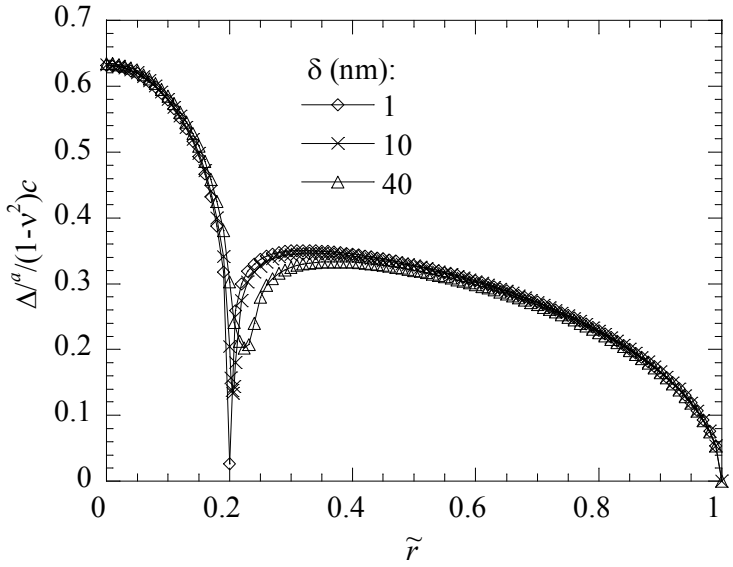

Figure 6. Crack opening of the penny crack under concurrent action of a droplet and a far-field tensile stress for three breadth widths (c=1 μm, a=c/5, σ_0=0.15E, θ=60°)